Impact of grid sensitivity and drag model along with the height of recirculating pipe on a cold flow circulating fluidized bed

Subham Kandel[*], Nirajan Raut[**], Niroj Koirala[*], Sunil Prasad Lohani[*], Britt M.E. Moldestad[**]

[*]*Department of Mechanical Engineering, Kathmandu University, Nepal*

(nepal.subham, ern.koirala)@gmail.com, splohani@ku.edu.np

[**]*Department of Process, Energy and Environmental Technology, University College of Southeast Norway, Norway*

[**]*nirajannraut@gmail.com, ([**]rajan.jaiswal, [**]britt.moldestad)@usn.no*

Abstract: Fluidized bed technology known for its efficient heat and mass transfer and controlled material handling, is widely used across industries. However, CFD simulation of fluidized beds presents challenges that require extensive validation. This study leverages the Multiphase Particle-In-Cell (MP-PIC) method, a recent Lagrangian modeling technique to improve computational efficiency and accuracy. The CAD model was developed using SolidWorks 2020 and simulation was carried out in the commercial CFD package Barracuda VR 21.1.0. The sensitivity of grid size, drag models and the impact of recirculating pipe height after loop seal was examined. Sand particles 63-200 μm and air were used as bed material and fluidization gas respectively achieving full flow circulation at 650 SL/min and 12 SL/min aeration in the riser and loop seal. A total of 19 different simulations were conducted, varying grid size and drag models each for a duration of 45 seconds with a time step of 0.0005 seconds. Pressure transducers along the CFB walls provided validation data. The Wen-Yu Ergun drag model showed a minimal error margin of 0.60%, followed by the Wen-Yu 80000 model at 0.62%, demonstrating high predictive accuracy.

Keywords: *Circulating Fluidized bed (CFB), Minimum fluidization velocity, CFD simulations, Time step, drag model, Multiphase particle-in-cell method, Grid size*

1. INTRODUCTION

Gas-solid fluidized bed technology is widely utilized in energy generation, pharmaceutical, chemical, petrochemical, electronic and metallurgical processing industries due to its distinct advantages of high heat and mass transfer and controlled material handling (Moradi *et al.*, 2020). Computational fluid dynamic (CFD) modeling has been identified as an excellent tool to produce information during the scaling up of pilot scale circulating fluidized beds to industrial scale. Further, it is a fast and cost-effective method for system optimization (Jaiswal *et al.*, 2022). CFD solves the conservation equations for mass, momentum, energy and species and this technique has been critically validated for accurate performance in gas or liquid single-phase flows. However, challenges remain related to interface coupling, solid-phase modeling and scale differences in gas-solid multiphase flow systems (Bandara *et al.*, 2016).

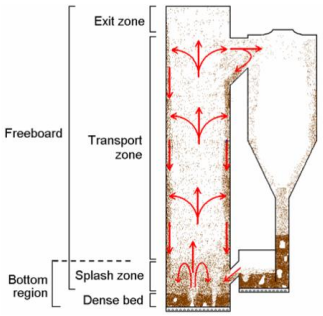

Fig. 1. Schematics of CFB (Pallarès, 2008).

Eulerian-Eulerian and Eulerian-Lagrangian are the two basic approaches for CFD modeling of multiphase flows. Multiphase Particle-In-Cell (MP PIC) modeling is a development of Eulerian-Lagrangian modeling and aims to reduce the computational cost in discrete modeling of the particle phase (Andrews and O'Rourke, 1996). Instead of tracking individual particles, it considers packets containing a certain number of particles with similar properties. The packets are modeled in the discrete phase while the particle phase interactions are modeled in an Eulerian frame (Snider *et al.*, 2001). Therefore, particle properties are calculated in both Eulerian and Lagrangian frames which are correlated via interpolation functions.

Validated CFD models can be used to analyze circulating fluidized beds in terms of particle circulation velocity, particle mixing and segregation (Bandara *et al.*, 2018). The conservation equations of mass species, momentum and energy are in partial differential form so the simulation geometry is divided into small cells referred to as the computational grid. The conservation equations are then discretized in space and time to form a set of algebraic equations (Bandara *et al.*, 2018). Finite difference, finite element and finite volume are the main techniques used with the finite volume method being most common for 3D systems involving mass, momentum and energy (Andrews and O'Rourke, 1996).

Errors and uncertainties are integrated from the modeling stage to the final computer simulations. The use of empirical equations and model simplification leads to deviations during

model development. Therefore, it is necessary to identify ways to reduce errors in simulations with minimal computational cost. This includes selecting the optimal drag model in gas-solid multiphase flow systems and conducting mesh sensitivity analysis to develop a grid independent model (Bandara *et al.*, 2018).

This paper investigates the impact of grid sensitivity and drag models alongside the height of the recirculating pipe after loop seal on the performance of cold flow circulating fluidized beds. Barracuda VR 21.1.0 was used to compare pressure data, varying grid size and drag model along with SolidWorks for CAD design. Through comprehensive CFD analysis, this study aims to enhance the accuracy and efficiency of circulating fluidized bed modeling for industrial applications.

2. MP PIC MODEL DESCRIPTION

The gas phase mass and momentum conservation can be modelled by the volume averaged Navier-Strokes equation and are used as a continuum on a Eulerian grid (Snider, 2001).

$$\frac{\partial(\theta_f \rho_f)}{\partial t} + \nabla.(\theta_f \rho_f u_f) = 0 \tag{1}$$

$$\frac{\partial(\theta_f \rho_f u_f)}{\partial t} + \nabla.(\theta_f \rho_f u_f) = \nabla p - F + \theta_f \rho_f g + \nabla.(\theta_f \tau_f) \tag{2}$$

$$F = \iint f m_s \left[D_s(u_f - u_s) - \frac{1}{\rho_s}\nabla p \right] dm_s du_s \tag{3}$$

where θ_f, ρ_f, u_f, τ_f are fluid phase volume fraction, density, velocity and stress tensor and m_s, u_s are the mass and velocity of the particle. F is the total momentum exchange with particle phase per volume, g is the acceleration due to gravity and p is the pressure.

The solid phase can be modelled by a particle distribution function given by equation 4 (O´Rourke *et al.*,2014). Considering the time rate of change of above equation the Liouville equation is obtained. This equation assumes that there are no direct collisions or particle breakup.

$$f(x, m_s, u_s, t) dm_s du_s$$

$$\frac{\partial f}{\partial t} + \nabla_x.(f u_s) + \nabla u_s.(f A) = 0 \tag{4}$$

The particle acceleration, A as a function of aerodynamics drag, buoyancy, gravity and interparticle normal stresses can be expressed as,

$$A = D_s(u_f - u_s) - \frac{1}{\rho_s}\nabla p + g - \frac{1}{\theta_s \rho_s}\nabla \tau_s \tag{5}$$

The particle volume fraction, θ_s and the particle stress τ_s, which are used to calculate the interparticle collisions and are expressed as (Rourke *et al.*, 2014)

$$\theta_s = \iint f \frac{m_s}{\rho_s} dm_s du_s \tag{6}$$

$$\tau_s = \frac{10 P_s \theta_s^{\beta}}{max\left[(\theta_{cp} - \theta_s), \epsilon(1 - \theta_s)\right]} \tag{7}$$

Here, P_s, β, θ_{cp} are the constant term related with pressure and is a constant, particle volume fraction equals the close pack volume.

3. METHOD AND COMPUTATIONAL MODEL

3.1 Experimental Model

The experiment was carried out at ambient temperature using sand particles with diameters ranging from 63 to 200 µm and a density of 2650 kg/m³. Prior to the experiment, particle size distribution analysis revealed a mean particle size of 116 µm. The gas flow rate in the riser was varied from 0 to 650 SLPM in increments of 50 SLPM and in the loop seal from 0 to 12 SLPM in increments of 2 SLPM. Pressure transducers were installed at various locations, with data acquisition managed through LabVIEW.

3.2 *Computational Model:*

Following the measurement of the dimensions of the CFB at the University of South-Eastern Norway, a CAD geometry was created using SOLIDWORKS 2020. The gas inlet of the riser and the loop seal were configured as flow boundary conditions, while the top of the cyclone was set up as a pressure boundary condition. The simulation time step was set to 0.0005 seconds (Bandara *et al.*, 2018), with a total simulation duration of 45 seconds. The maximum momentum from particle collision redirection was assumed to be 40%, and the default values of 0.85 were used for normal and tangential wall collisions.

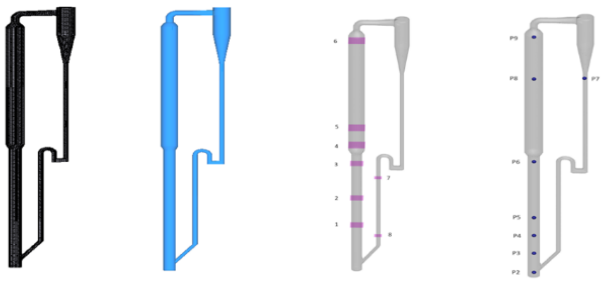

Fig. 2. (a) Grid (b) CAD Geometry (c) Flux Planes (d) Pressure reading Points.

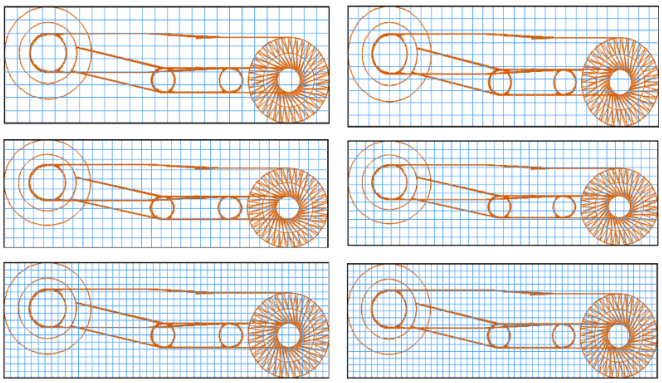

Fig. 3. Grid size with 40000, 60000, 80000, 120000, 240000, 300000 uniform grid size (Top left to bottom right).

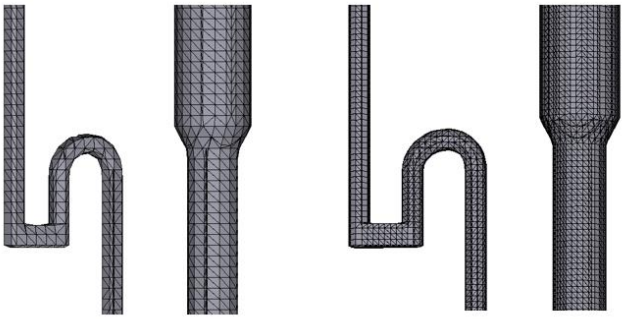

Fig. 4. CAD model with 40000 and 30000 uniform grid size.

4. RESULT AND DISCUSSION

4.1 Drag Model

Three different drag models Ergun, Wen-Yu and a combined Wen-Yu Ergun model were evaluated to accurately compare the computational results with the experimental data.

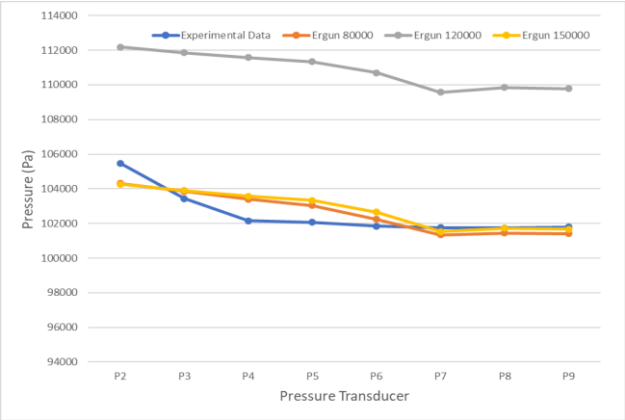

Fig. 5. Ergun drag model with different grid size

In the above study, the Ergun model was analyzed using different grid sizes. When increasing the grid size from 80,000 to 150,000 cells it was observed that a grid size of 120,000 cells resulted in greater deviation, whereas grid sizes of 80,000 and 150,000 cells closely matched the experimental data. The average deviations for grid sizes of 80,000, 120,000 and 150,000 cells were 0.69%, 8.12% and 0.67% respectively as shown in Fig. 5. These results clearly indicate that the Ergun model with grid sizes of 80,000 and 150,000 cells provides accurate predictions for our experimental model.

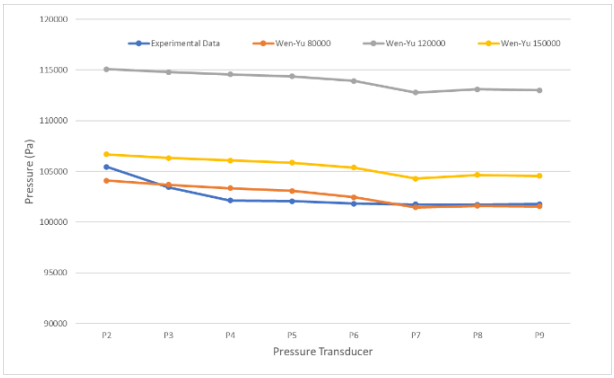

Fig. 6. Wen-Yu drag model with different grid size.

In the above analysis, the Wen-Yu model was evaluated using different grid sizes. As the grid size was increased from 80,000 to 150,000 cells, it was observed that the 120,000 cell exhibited the highest deviation followed by the 150,000 cell whereas the 80,000 cell provided accurate predictions compared to the experimental data. The average deviations for the 80,000, 120,000 and 150,000 grid cells were 0.62%, 11.15% and 2.88% respectively as shown in Fig. 6. These results clearly indicate that the Wen-Yu model with a grid size of 80,000 cells offers the best prediction accuracy for our experimental model.

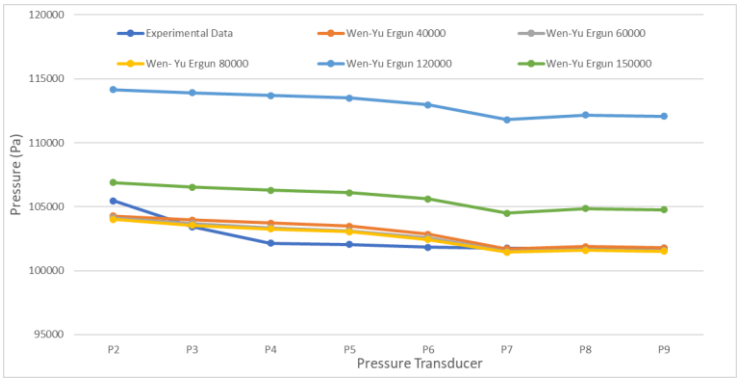

Fig. 7. Wen-Yu Ergun drag model with different grid size.

In the above study, the Wen-Yu Ergun model was evaluated using various grid sizes. Increasing the grid size from 40,000 to 150,000 cells revealed that grids of 120,000 and 150,000 cells exhibited greater deviation, while grids of 40,000, 60,000 and 80,000 cells closely matched the experimental data. The average deviations for grid sizes of 40,000, 60,000, 80,000, 120,000 and 150,000 cells were 0.71%, 0.62%, 0.60%, 10.25% and 3.09% respectively as shown in Fig. 7. These result clearly indicates that the Wen-Yu Ergun model with a grid size of 80,000 cells provides the most accurate predictions for our experimental model.

4.2 Grid Size

Different grid sizes ranging from 40,000 to 300,000 were tested for grid independence test with three different drag models and the results are presented below.

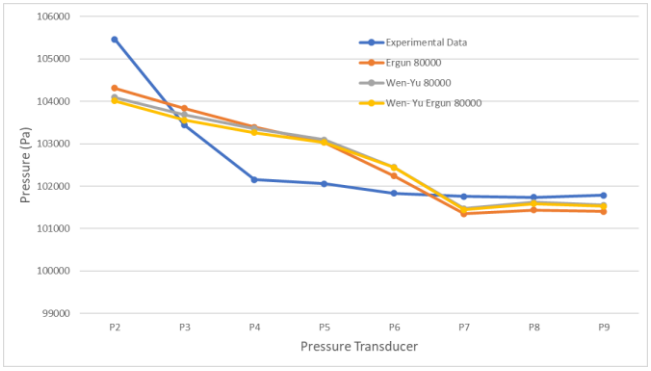

Fig. 8. Different drag model with 80000 grid size.

In this study, the Wen-Yu Ergun drag model with an 80,000 grid cells accurately predicted the experimental setup. The errors for the Ergun, Wen-Yu, and Wen-Yu Ergun models were 0.63%, 0.62% and 0.60%, respectively as shown in Fig. 8.

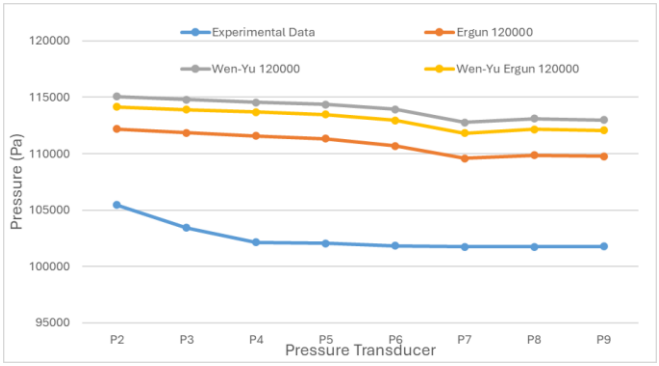

Fig. 9. Different drag model with 150000 grid size.

In the above study, increasing the grid size resulted in greater deviation. The deviation is smallest for the Ergun followed by the Wen-Yu Ergun and is highest for the Wen-Yu model. The errors for the Ergun, Wen-Yu and Wen-Yu Ergun model are 8.12%, 11.15% and 10.25% respectively as shown in Fig. 9.

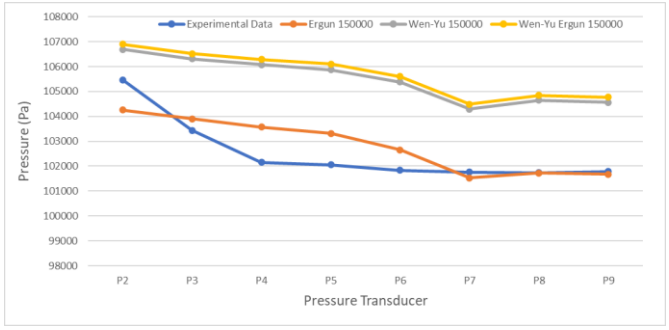

Fig. 10. Different drag model with 300000 grid size.

In the above study, increasing the grid size led to greater deviation. The Ergun model exhibited the least deviation followed by the Wen-Yu and Wen-Yu Ergun models. The deviation for these drag models with the specified grid sizes are 0.67%, 2.88% and 3.09% respectively as shown in Fig. 10.

4.3 Impact of height of recirculating pipe after loop seal on recirculation rate

Increasing the height of the recirculating pipe after the loop seal in a circulating fluidized bed (CFB) system significantly impacts particle recirculation rate and system performance. The height affects gravitational forces, particle velocity and settling behavior. A taller recirculating pipe increases pressure drop and alters particle flow dynamics potentially reducing velocities if not compensated for the increased gravitational and pressure effects.

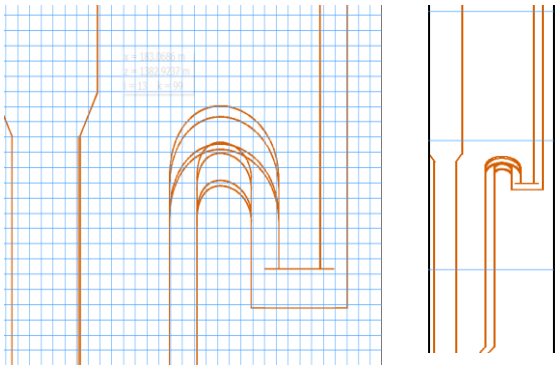

Fig. 11. CAD model with varying recirculating pipe height.

Length and Height of Recirculating Pipe		
Height (mm)	Circulation Rate (kg)	Change in Circulation Rate
(950-43)	1.31	7.38
(955-48)	1.16	-4.92
(960-53)	1.2	-1.64
(965-58)	1.26	3.28
(970-63)	1.22	0.00
(975-68)	1.15	-5.74
(980-73)	1.08	-11.48
(985-78)	1.1	-9.84
(990-83)	1.08	-11.48

In the design, nine modifications were made varying the recirculating height from 950 mm to 990 mm, with the original height being 970 mm. These changes also affect the height just after the loop seal. A greater height requires more pressure for sand transfer to the riser while a lower height facilitates particle flow from the riser to the loop seal.

In nine simulations, the configuration with a 965 mm height and 58 mm height just after the loop seal achieved the highest recirculation rate as shown in Figs. 12 and 13. Initially the 950 mm configuration had the highest rate up to 45 seconds, but the (965-58) mm configuration provided the best circulation rate over a 300 second simulation.

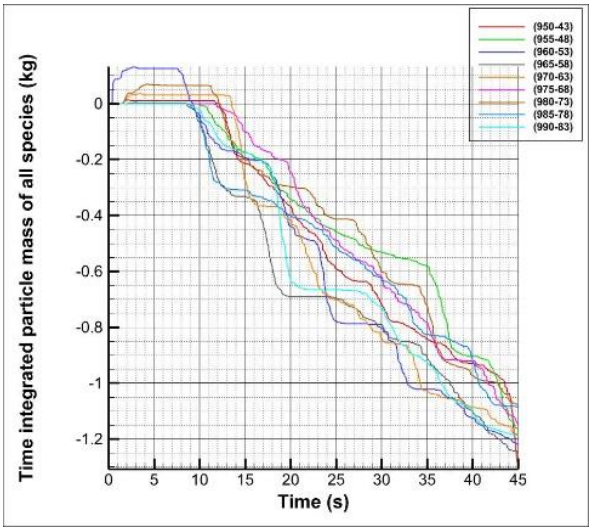

Fig. 12. Particle circulation rate with different height of recirculating pipe (45 seconds).

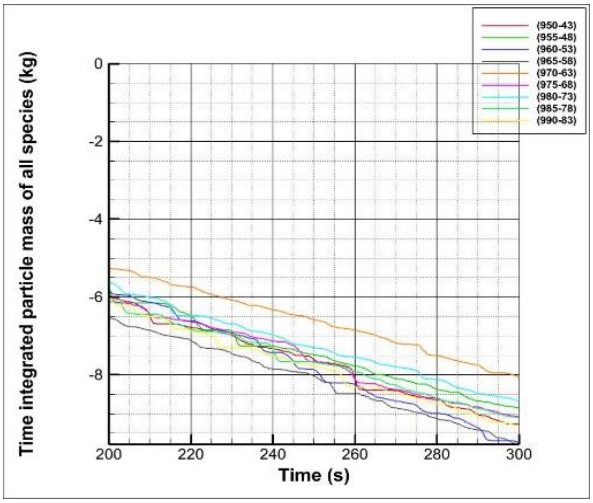

Fig 13. Particle circulation rate with different height of recirculating pipe (300 seconds).

5. CONCLUSION

This study investigates the impact of drag model and grid size on the accuracy of experimental and computational models in a cold flow circulating fluidized bed (CFB) system. Sand particles ranging from 63-200 μm were used as the bed material with air as the fluidizing agent. The minimum airflow for particle circulation was determined experimentally and was found to be 650 SLPM in the riser and 12 SLPM in the loop seal.

Analysis reveals that the Wen-Yu Ergun model with a grid size of 80,000 accurately represents the experimental model computationally. Accuracy improves progressively from 40,000 to 80,000 grid size peaking at 80,000 before declining beyond this threshold. Conversely, when the same model is analyzed with a higher grid size of 300,000, the deviation increases to 11.17%. This deviation is attributed to particle size becoming smaller than the grid size beyond 80,000.

Furthermore, the circulation rate is observed to be highest for the (965-58) mm configuration compared to the (970-63) mm model used in the experiment. This is because greater height necessitates more pressure for sand transfer to the riser, while lesser height facilitates more particle flow from the riser to the loop seal. Insufficient height leads to suboptimal particle circulation due to pressure pushing particles from the loop seal towards the standpipe.

In conclusion, drag model and grid size significantly impacts computational accuracy, with no one particular model applicable across all CFB models. Additionally, particle characteristics play a crucial role in model validation with uniform particle size essential for accurate predictions. Moreover, the height of the recirculating pipe profoundly influences particle circulation rate, emphasizing the importance of designing an optimal height for efficient operation of circulating fluidized beds.

REFERENCES

Andrews, M. J., and O'Rourke, P. J. (1996). THE MULTIPHASE PARTICLE-IN-CELL (MP-PIC) METHOD FOR DENSE PARTICULATE FLOWS. Pergamon Int. J. Multiphase Flow, 22(2).

Bandara, J. C., Nielsen, H. K., Moldestad, B. M. E., and Eikeland, M. S. (2018). Sensitivity Analysis and Effect of Simulation parameters of CPFD Simulation in Fluidized Beds. Proceedings of The 59th Conference on Simulation and Modelling (SIMS 59), 26-28 September 2018, Oslo Metropolitan University, Norway, 153, 334–341.

Bandara, J. C., Thapa, R. K., Moldestad, B. M. E., and Eikeland, M. S. (2016). Simulation of Particle Segregation in Fluidized Beds. Proceedings of The 57th EUROSIM Congress on Modelling and Simulation, EUROSIM 2016, The 57th SIMS Conference on Simulation and Modelling SIMS 2016, 142, 991–997.

Huang, Y. (2024). Dynamic model of circulating fluidized bed. https://researchrepository.wvu.edu/etd/2749

Jaiswal, R., Eikeland, M. S., Moldestad, B. M. E., and Thapa, R. K. (2022). Influence on the fluidization pattern of a freely bubbling fluidized bed with different modes of air supply. Proceedings of the 63rd International Conference of Scandinavian Simulation Society, SIMS 2022, Trondheim, Norway, September 20-21, 2022, 192, 291 –296.

Moradi, A., Samani, N. A., Mojarrad, M., Sharfuddin, M., Bandara, J. C., and Moldestad, B. M. E. (2020). Experimental and computational studies of circulating fluidized bed. International Journal of Energy Production and Management, 5(4), 302 –313.

Pallarès, David., and Chalmers tekniska h ögskola. Department of Energy and Environment. Division of Energy Technology. (2008). Fluidized bed combust ion : modeling and mixing. Chalmers University of Technology.

O'Rourke, P. J., and Snider, D. M. (2014). A new blended acceleration model for the particle contact forces induced by an interstitial fluid in dense particle/fluid flows, Powder Technology, 256, 39–51,

Snider, D. M. (2001). An Incompressible Three-Dimensional Multiphase Particle-in-Cell Model for Dense Particle Flows, Journal of Computational Physics, 170(2), 523–549.